Readaptation of mesenchymal stem cells to high stiffness and oxygen environments modulate the extracellular matrix

Inês Caramelo[1,2,3], Catarina Domingues[1,3,4], Vera M. Mendes[1,3], Sandra I. Anjo[1,3,4], Margarida Geraldo[1], Carla M. P. Cardoso[3,5], Mário Grãos[3,6], Bruno Manadas[1,3,4]

[1] CNC-Center for Neuroscience and Cell Biology, University of Coimbra, 3004-504 Coimbra, Portugal;

[2] PhD Programme in Experimental Biology and Biomedicine, Institute for Interdisciplinary Research (IIIUC), University of Coimbra, Casa Costa Alemão, 3030-789 Coimbra, Portugal

[3] CIBB - Centre for Innovative Biomedicine and Biotechnology, University of Coimbra

[4] Institute for Interdisciplinary Research, University of Coimbra (IIIUC), 3030-789 Coimbra, Portugal;

[5] Stemlab, S.A. (Crioestaminal), 3060-197 Cantanhede, Portugal

[6] Biocant, Technology Transfer Association, 3060-197 Cantanhede, Portugal

Graphical Abstract

Abstract

The therapeutic potential of mesenchymal stem cells (MSCs) has been explored over the past decades due to their ability to modulate the microenvironment through paracrine signaling. Consequently, the secretome of MCSs has emerged as a cell-free therapy rather than a cell therapy, offering the advantages of being readily commercialized as an off-the-shelf product without immunogenicity compatibility issues. As a result, strategies to manipulate and enhance the secretory profile of MSCs' secretome are emerging. MSCs from the Wharton's jelly niche are accommodated to the stiffness and oxygen level found at the umbilical cord (UC), which are 2 to 5kPa (Young's modulus) and

2.4% to 3.8% O_2, respectively. However *in vitro* culture conditions (2-3 GPa and 18.5% O_2) are largely different from the one observed in vivo. Here, we present a proteomic characterization of the secretome of MSCs primed (48h) or readapted (7-10 days) to soft (3kPa) (mechanomodulated) or low oxygen levels (5% O_2) (physioxia). Maintaining MSCs on soft platforms for long periods increased the secretion of proteins associated with cell redox homeostasis, such as protein disulfide isomerases and mitochondrial proteins, while physioxia enhanced the secretion of immunomodulatory proteins. The high secretion of these proteins might confer a therapeutical advantage by favoring a regenerative environment at the injury site. Interestingly, lowering the stiffness or oxygen converged on the downregulation of several extracellular matrix proteins (ECM), particularly collagen fibrils, on primed and readapted cells. These results suggest that a massive reorganization of the extracellular space occurs upon culturing MSCs on conventional culture conditions, which may affect not only matrix stiffness but also several signaling pathways initiated at the cell membrane, such as PDGF signaling pathways (e.g., PI3K-AKT), consequently biasing stem cell fate. In conclusion, mimicking physiological culture conditions *in vitro* modulates secretome composition, which may empower its therapeutical properties by enriching proteins that promote cell survival.

Keywords

Mesenchymal stem cells; Extracellular matrix; Secretome; Mechanomodulation; Physioxia; Proteomics

Introduction

The therapeutic potential of mesenchymal stem cells (MSCs) has gathered significant attention in the regenerative medicine field (1). These cells exhibit the capability not only to self-renewal *in vitro* but also to differentiate into multiple lineages, making them suitable for a broad spectrum of clinical applications (2, 3). For many years, MSCs treatments comprised mainly the autologous or allogenic transplantation of cells (“cell-based therapy”) (4). While the former is described to have lower associated risks, recent clinical trials have

shown that allogenic MSCs are also a safe and promising treatment approach (5, 6). Once administered, MSCs are chemoattracted to the injury site, where they promote tissue repair (1, 7). Beyond their regenerative role through the differentiation and replacement of damaged cells, MSCs are renowned for their ability to modulate the microenvironment through paracrine signaling, highlighting the increasing importance of this fluid in regenerative medicine (8).

Recent studies have used the secretome of MCSs as a “cell-free therapy”. The secretome is the collection of bioactive substances secreted by cells into the extracellular space and can be categorized into two main parts: the soluble fraction, containing growth factors and cytokines, among others, and the vesicular fraction, which includes exosomes and larger vesicles (8, 9). These components can modulate different processes in the surrounding cells, such as immunomodulation, apoptosis, angiogenesis, and antioxidation (8, 10). As a result, the secretome administration is emerging as an alternative to cell therapy. This approach offers numerous advantages, particularly in terms of safety, since it avoids immunogenicity and compatibility issues and is more comparable to conventional pharmaceutical products in terms of dosage and potency (11, 12). Additionally, it can be readily commercialized as an off-the-shelf product, with extended storage lifespans without compromising potency, and is more easily scalable, thus making it financially viable. However, the secretome composition is highly dynamic and can vary depending on the MSCs source and in response to subtle different culture conditions (13, 14), which can affect consistency between batches.

Recently, strategies to manipulate and enhance the secretory profile of MSCs secretome have been explored. These approaches involve either culturing these cells on 2D or 3D hydrogels with customized biochemical and biophysical properties, using priming strategies by adding drugs and soluble factors, such as cytokines, or replicating hypoxic environments (15, 16).

MSCs can sense and respond to biophysical properties of the surrounding environment, including stiffness and tissue oxygen levels (17, 18). For instance, MSCs at the Wharton’s jelly niche respond to the stiffness and oxygen level found at the umbilical cord (UC), which is 2 to 5kPa (Young’s modulus) and 2.4% to 3.8% O_2, respectively (19, 20). To replicate these physiological conditions *in vitro,* we previously optimized culture conditions for MSCs on

softer polydimethylsiloxane (PDMS) platforms (~3kPa) or under controlled oxygen levels (~5% O_2) (21). The proteomic characterization unveiled alterations at the cellular level and a differential expression of extracellular matrix (ECM) proteins, suggesting that the secretory profile of these MSCs might also be altered in response to these physiological cues. In this study, we provide a proteomic analysis of the secretome of MSCs isolated from the umbilical cord (UC-MSCs) cultured on 3kPa platforms (mechanomodulated) and exposed to controlled levels of oxygen (5% O_2, physioxia) for 7-10 days (readapted) or 48 hours (primed).

Methods

Cell culture

Isolation and expansion of UC-MSCs

Experiments were performed as previously described (21, 22). All the procedures were approved by the Ethics Committee of the Faculty of Medicine, University of Coimbra, Portugal (ref. CE-075/2019). Briefly, MSCs were isolated from fragments from the UC matrix (Wharton's jelly) and expanded with proliferation medium (Minimum essential Medium-α (MEM-α) (Gibco™) supplemented with 10% (v/v) MSC-qualified fetal bovine serum (FBS) (Hyclone, GE Healthcare) (only for readapted mechanomodulated MSCs) or 5% (v/v) fibrinogen depleted human platelet lysate (HPL) (UltraGRO™, Helios) and antibiotics: 100 U/ml of Penicillin, 100 µg/ml Streptomycin and 2.5 µg/ml Amphotericin B or Antibiotic-Antimycotic (all from Gibco™). When cells were confluent, MSCs were trypsinized by adding 0.05% Trypsin-EDTA solution (Gibco™) for five minutes at 37ºC, homogenized, centrifuged, and seeded at the desired density.

For standard culture conditions, UC-MSCs were kept on a humidified incubator at 37ºC, with 5% CO_2, on a tissue culture polystyrene (TCP) dish, from P2 to P4. For priming experiments, cells were seeded at 10.000/cm^2 (P4).

MSCs expansion under physiological culture conditions

Two different physiological environments were created separately: low stiffness or oxygen levels. Mechanomodulated MSCs were kept under low stiffness conditions (3kPa). To create soft culture conditions, platforms of polydimethylsiloxane (PDMS) were prepared and functionalized as previously described (22). Physioxia MSCs were maintained in a low oxygen environment. For that, MSCs were cultured in an InvivoO_2® 400 Physoxia Workstation (Baker), with 5% O_2, 5% CO_2 and humidified environment, in accordance with the protocol previously described (21).

For both experimental conditions, UC-MSCs were expanded under conditions that mimic a physiological environment (3kPa platforms or 5%O_2) for 7-10 days, as the population doubling depends on the donors, (hereafter termed "re-adapted") or for 48h (termed "priming"). To prepare the conditioned medium (CM), UC-MSCs were washed twice with PBS, and a fresh culture medium without supplements (only antibiotics) was added. This procedure aims to remove supplemented proteins, which, owing to their high abundance, might compromise the detection of secreted proteins due to their low abundance. UC-MSCs were left to secrete for 48h (readapted) or 24h (priming).

Proteomic analysis

Secretome preparation

The secretome was prepared as previously described (23). Briefly, CM was collected and centrifuged at 290×g for 5 min at 4ºC. The 4µg of protein standard (MBP-GFP) was added to the same volume of secretome (24). Then, the supernatant was transferred to a low molecular weight cut-off (5kDa Vivaspin® 20, Sartorius) and centrifuged at 3,000×g, at 4ºC, until the desired concentration was achieved. Then, proteins were precipitated through the sequential addition of trichloroacetic acid and acetone and resuspended on sample buffer 2× (116.7 mM Tris- HCl pH 6.8, 10% (v/v) Glycerol, 3.3% (w/v) SDS, 0.31% (w/v) dithiothreitol (DTT), bromophenol blue).

For the proteomic analysis, the total volume of CM was analyzed, except for physioxia readapted secretome, where an equal amount of protein was loaded in the gel (50µg). Proteins were first alkylated by the addition of a 40% (w/v) acrylamide solution and resolved through a short-GeLC approach and stained

with Coomassie Brilliant Blue G-250 (25, 26). Pools of each condition were prepared for protein identification. Concerning protein quantification, each sample was loaded individually. Gel lanes were cut and destained, and proteins were digested overnight in gel using trypsin. Finally, the peptides were extracted through the sequential addition of solutions with increasing acetonitrile concentration (30%, 50% and 98%) and 1% formic acid, dried by vacuum centrifugation at 60°C, and stored at -20°C.

Data acquisition

Samples were analyzed as previously described (21). Briefly, samples were resuspended in a solution of 2% acetonitrile and 0.1% formic acid and analyzed using a NanoLC™ 425 System (Eksigent) coupled to a Triple TOF™ 6600 mass spectrometer (Sciex) equipped with an electrospray ionization source (DuoSpray™ Ion Source from Sciex). Peptides were separated on a Triart C18 Capillary Column 1/32" (12 nm, 3 µm, 150 mm × 0.3 mm, YMC) and using a Triart C18 Capillary Guard Column (0.5 mm × 5 mm, 3 µm, 12 nm, YMC) at 50 °C. The flow rate was set to 5 µL/min and mobile phases A and B were 5% DMSO plus 0.1% formic acid in water and 5% DMSO plus 0.1% formic acid in acetonitrile, respectively. The LC program was performed as follows: 5 - 30% of B (0 - 50 min), 30 - 98% of B (50 - 52 min), 98% of B (52-54 min), 98 - 5% of B (54 - 56 min), and 5% of B (56 - 65 min). The ionization source was operated in the positive mode set to an ion spray voltage of 5500 V, 25 psi for nebulizer gas 1 (GS1), 10 psi for nebulizer gas 2 (GS2), 25 psi for the curtain gas (CUR), and source temperature (TEM) at 100°C. For Data Dependent Acquisition (DDA) experiments, the mass spectrometer was set to scan full spectra (m/z 350-2250) for 250 ms, followed by up to 100 MS/MS scans (m/z 100-1500) with a 30 ms accumulation time, resulting in a cycle time of 3.3 s. Candidate ions with a charge state between + 1 and + 5 and counts above a minimum threshold of 10 counts per second were isolated for fragmentation, and one MS/MS spectrum was collected before adding those ions to the exclusion list for 15 s (mass spectrometer operated by Analyst® TF 1.8.1, Sciex). For Data Independent Acquisition (DIA) (or Sequential Window Acquisition of all Theoretical Mass Spectra (SWATH)) experiments, the mass spectrometer was operated in a looped product ion mode and specifically tuned to a set of 42 overlapping

windows, covering the precursor mass range of 350–1400 m/z. A 50 ms survey scan (m/z 350–2250) was acquired at the beginning of each cycle, and SWATH-MS/MS spectra were collected from 100 to 2250 m/z for 50 ms, resulting in a cycle time of 2.2 s.

Data analysis

The five fractions of each pool were acquired individually in DDA mode. To generate the ion library, all files were combined and searched against the reviewed Human (Swiss-Prot) database (downloaded on 21st October 2021 (for re-adapted MSCs experiments) and 16th May 2022 (for priming) using the ProteinPilot™ software (v5.0, Sciex). An independent False Discovery Rate (FDR) analysis was performed using the target-decoy approach provided by the software to assess the quality of the identifications. Concerning protein relative quantification, samples were acquired on DIA mode (SWATH) and analyzed individually. Data processing was performed using the SWATH™ plug-in for PeakView™ (v2.0.01, Sciex), configured to select up to 15 peptides per protein and five transitions per peptide. To avoid the interference of FBS contaminants on long exposure mechanomodulation experimental setup, a sequence list of highly abundant fetal bovine serum proteins was added to the database (27). These proteins were removed from the analysis.

Peptides were only quantified if they had an FDR below 1% in at least one-third of the samples per condition and were normalized to the total intensity of the sample. The MS data have been deposited to the ProteomeXchange Consortium via the PRIDE partner repository with the dataset identifier PXD052907. *Credentials for reviewers only: Username: reviewer_pxd052907@ebi.ac.uk Password: sXN2pzxkN24C*

MetaboAnalyst 5.0 online platform and GraphPad Prism 9 were used to perform the statistical analyses (28). Both univariate (t-test or Mann-Whitney or Kruskal-Wallis tests) and multivariate (Partial least squares-discriminant analysis (PLS-DA)) analyses were used to identify proteins of interest. Hits were selected if they had a VIP>1, $p<0.05$, or both, and fold change (FC) above 1.5 or below 0.67 ($|Log_{1.5}FC|>1$) for further analysis. FunRich was used to perform a Gene Ontology (GO) enrichment analysis (29), while pathways were mapped using the Reactome database (30). Pathways were searched on KEGG database

(31). Violin plots were created on GraphPad Prism 9 and Venn diagrams were generated on DeepVenn (32).

Results

Readapting UC-MSCs to low stiffness or oxygen environments modulates their secretory profile

MSCs can act through paracrine signaling to promote tissue regeneration at the site of injury; therefore, unveiling the composition of their secretome has emerged as a hot topic in this research field. Previous data indicated that culturing MSCs on lower stiffness platforms modulated the cellular proteome, including components of the extracellular matrix (21, 22). Therefore, it was hypothesized that the secretome composition might also be altered in response to mechanical cues. Hence, UC-MSCs were expanded on 3kPa platforms (P2-P4), and the CM was collected and subjected to a proteomic analysis. From the 1007 proteins identified, 705 proteins were quantified with confidence and subjected to statistical analysis to identify significantly secreted proteins under a low stiffness environment, compared to standard culture conditions. The PLS-DA scores plot showed no overlap between the two experimental groups (Figure 1A). Additionally, using a univariate approach, several proteins were identified as more or less abundant (Figure 1B). Next, the 193 significant proteins (VIP>1, $p<0.05$, or both, and $|Log_{1.5}FC|>1$) were subjected to a GO analysis. Looking at the biological processes, upregulated proteins are mainly associated with carbohydrate metabolism, cell redox homeostasis, and protein folding processes (Figure 1C). In contrast, proteins associated with translation and extracellular matrix organization cell adhesion decrease in the CM of UC-MSCs kept in soft platforms.

To evaluate if the secretory profile rate was being altered, UC-MSCs, the proteome of both the cellular (previously published (21)) and secretome fractions was compared, where 11.2% and 13.3% of the proteins where found to be up- and down-regulated on both fractions, respectively (Figure 1D). Proteins found to be decreased both on the cellular proteome and secretome

were mainly involved in the protein metabolism (e.g., translation), RNA processes (e.g., rRNA processing), and ECM organization (e.g., collagen formation) (Figure 1E, Supplementary Table 1). On the other hand, cellular carbohydrate metabolism also appears to be the main mechanism altered when considering upregulated proteins since the levels of several proteins associated with the citric acid (TCA) cycle, respiratory electron transport, and mitochondrial biogenesis increased when cells were readapted to low stiffness environments (Figure 1F, Supplementary Table 2). Besides, proteins commonly upregulated were found to be associated with cell detoxification of reactive oxygen species (ROS) processes Only a few proteins (10 out of 490 proteins) exhibit an opposite profile when comparing the cellular proteome and secretome, suggesting that these proteins might either be more secreted to the extracellular environment or accumulate inside the cell, decreasing the secretion in response to the physiological environment (Supplementary Figure 1A-B, respectively).

The overall results suggest that when UC-MSCs are exposed to prolonged periods in culture conditions with low stiffness, the composition of the secretome changes. This may be due to an alteration in protein abundance inside the cell and the maintenance of secretion rates or a result of regulation of the secretion rate in response to the extracellular environment.

Figure 1 – *Proteins involved in carbohydrate, RNA, and protein metabolism and ECM are differentially secreted by MSCs readapted to low stiffness conditions.* All quantified proteins on both standard (grey) and mechanomodulation (green) groups were used to generate a PLS-DA scores plot (A). The statistically different proteins (t-test, $p<0.05$; $|Log_{1.5}FC|>1$) are highlighted on the Volcano Plot (upregulated in green; downregulated in blue) (B). In total, 121 and 72 significant proteins were found to be down- (↓) or up- (↑) regulated, respectively (VIP>1, $p<0.05$, or both; $|Log_{1.5}FC|>1$). These proteins were subjected to a GO analysis. Significant biological processes (GO) are represented (circles for downregulated and triangles for upregulated proteins) (C). Next, differentially expressed proteins of the proteome and secretome were compared (D). Common proteins shared by both fractions were then analyzed. The most significant Reactome pathways of the commonly forty down- and nineteen up-regulated proteins are highlighted in yellow (E and F, respectively; Supplementary Tables 1 and 2). Abbreviations: Benjamini-Hochberg method (BH).

Previous data reported that UC-MSCs cellular proteome was altered when cells were maintained under physiological oxygen levels, particularly interfering with protein metabolism processes (21). To investigate if changes in these processes impacted UC-MSCs' secretory profile, the CM of UC-MSCs readapted to physioxia (5% oxygen) was explored. After expansion under low oxygen levels (7 to 10 days), the CM of UC-MSCs was collected for proteome

analysis using the above-mentioned pipeline. The generated library comprised 1535 proteins identified with confidence, from which 450 proteins were quantified with confidence (SWATH-MS). To identify interesting targets, all quantified proteins underwent a univariate and multivariate analysis approach. The two experimental groups do not intersect on the PLS-DA scores plot (Figure 2A). In addition, the volcano plot highlights significant up- and downregulated proteins (Figure 2B). To disclose the biological processes in which proteins of interest play a role, these proteins were subjected to a GO analysis. Data revealed that upregulated proteins are mainly associated with fibrinolysis and innate and adaptative immune responses. In contrast, proteins of the extracellular matrix and involved in cell adhesion processes appear to be downregulated (Figure 2C, Supplementary Table 3).

Next, the protein levels of the cellular proteome and secretome were compared to identify trends in secretion profiles modulated by physioxia oxygen levels culture conditions, with 5.3% of the proteins found to be commonly increased on both fractions, while 7.0% were decreased (Figure 2D). Proteins associated with extracellular matrix organization, mainly collagen, elastic fibers, and fibronectin components, are downregulated both in the intra and extracellular environment (Figure 2E, Supplementary Table 4). Moreover, the metabolism of glycosaminoglycans and post-translational modifications of proteins, including phosphorylation and calnexin/calreticulin cycle, were also described to be downregulated. Conversely, proteins associated with innate immune responses were increased in both proteome and secretome, as well as proteins involved in forming the fibrin clot (hemostasis) and scavenging the heme from the plasma (Figure 2F, Supplementary Table 5). Finally, four proteins lyase display inverse tendencies on both fractions, suggesting that the cellular levels of these proteins might be influenced by increased or decreased secretory rates or altered vesicle transport dynamics, including internalization processes (Supplementary Figure 1C-D).

Figure 2 – *Readapting MSCs to low oxygen environments modulates the secretion of proteins involved in metabolism, the immune system, and ECM.* The PLS-DA scores plot (A) represents all quantified proteins. The Volcano Plot highlights significant proteins up- (↑) (green) and down- (↓) (blue) regulated (t-test,

p<0.05; $|Log_{1.5}FC|>1$) (B). Data analysis revealed that 120 and 122 proteins were down- (↓) and up- (↑) regulated, respectively (VIP>1, p<0.05, or both; $|Log_{1.5}FC|>1$). (C) Biological processes (GO) of these proteins (BH method, p<0.001; all significant hits are available in Supplementary Table 3). The statistically altered proteins for the secretome and previously published cellular fraction (21) were compared (D). Proteins highlighted in the intersections were further explored. Significant Reactome pathways of the thirty down- and fifteen up-regulated proteins shared by both screenings are represented in yellow (E and F, respectively; Supplementary Tables 4 and 5). Abbreviations: Benjamini-Hochberg method (BH).

Extracellular matrix (ECM) proteins play a key role in the adaptation of UC-MSCs to physiological environments

Data analysis revealed that mimicking the physiological stiffness and oxygen levels environment *in vitro* led to a modulation of the extracellular matrix organization, cell adhesion, and the metabolism of proteins. To explore common mechanisms shared by these physiological-like environments, statistically different proteins previously described for both screenings were compared (Figure 3A). Only ATP synthase subunit alpha (mitochondrial) was found to be upregulated in both conditions (Supplementary Figure 1E). However, the levels of Talin-1, a protein involved in cell-matrix interaction, increased on physioxia-modulated secretome and decreased on mechanomodulated secretome (Supplementary Figure 1F). The majority of common proteins was found to be downregulated when MSCs were readapted to low oxygen or stiffness environments. The role of these proteins was further explored using Reactome database. Results indicate that these proteins are associated with the extracellular matrix organization, namely collagen, and proteins involved in the cross-linking of these fibrils, as peroxidasin homolog, and proteoglycans, as well as some proteins involved in MET (Hepatocyte growth factor receptor) or PDGF (Platelet-Derived Growth Factor) signaling pathways (Figure 3B, D, Supplementary Table 6). In addition, the ten proteins with inverse tendencies in both physiological environments were found to be involved in glucose metabolism and protein post-translational modifications, particularly affecting the calnexin/calreticulin cycle (Figure 3F and Supplementary Figure 1G, Supplementary Table 7). It can be concluded that similarly to what has been observed for the cellular proteome (33), the two different physiological environments culminate in the diminished secretion of common proteins, particularly ECM proteins.

Figure 3 – UC-*MSCs kept under low stiffness or oxygen levels conditions commonly reorganize the secretion of ECM proteins.* Significant proteins previously selected (VIP>1, p<0.05, or both; $|Log_{1.5}FC|>1$) from each screening were compared and are represented on the Venn diagram (A). Proteins shared by both experimental conditions were further analyzed. Significant Reactome pathways of the twenty-eight proteins commonly downregulated under physiological conditions (B) and the ten proteins upregulated by mechanomodulation and downregulated by physioxia (C) are represented in yellow (details can be consulted in Supplementary Tables 6 and 7). In detail, the proteins involved in the PDGF signaling (that can activate PI3K/AKT signaling pathway) (D) are highlighted in circles, according to the Kegg Pathway database (grey: proteins that belong to the pathway; light green: downregulated on mechanomodulation; light brown: downregulated on physioxia). Abbreviations: COL4A1: collagen type IV alpha 1 chain; COL6A3: collagen type VI alpha 3 chain; THBS2: thrombospondin 2; ITGA: integrin subunit alpha; ITGB: integrin beta; FAK: protein tyrosine kinase 2; PI3K: phosphatidylinositol-4,5-bisphosphate 3-kinase catalytic subunit alpha; PIP_3: phosphatidylinositol-3, 4, 5-triphosphate; AKT: AKT serine/threonine kinase 3)

Expanding UC-MSCs under standard culture conditions for long periods (7-10 days) does not impair UC-MSCs' ability to adapt to lower stiffness and oxygen culture conditions, as previously published (21). Therefore, it was hypothesized that the secretory profile of MSCs was able to adapt to physiological environments for a short period after being expanded at standard conditions – priming. Briefly, UC-MSCs were expanded under standard culture conditions until passage 3, after which cells were primed for 48h, using low stiffness platforms (3kPa) or a physioxia environment (5% O_2) or maintained in standard conditions. Then, primed UC-MSCs secretome was collected, and the proteome was analyzed as previously. This resulted in the identification of 557 proteins, from which 413 were quantified with confidence in all experimental groups. The cluster analysis and the PCA scores plot demonstrate a closer relationship between the standard and physioxia secretome despite the separation of the three groups on the PLS-DA model (Figure 4A and Supplementary Figure 2A-B, respectively). Next, the GO analysis revealed that keeping cells on low-stiffness platforms decreases the secretion of proteins involved in cell adhesion, more specifically, various types of collagen, as described in long-exposure experiments (Figure 4B, 1C, and Supplementary Figure 2D). In parallel, physioxia priming upregulates proteins associated with immunomodulatory responses, as observed in long-exposure experiments Figure 4B and Supplementary Figure 2D). Interestingly, the extracellular matrix components, particularly the collagen fibril organization, were found to be downregulated upon both physiological priming, consistent with the secretory profile of readapted MSCs. Together, this data suggests that the extracellular matrix is a key player in adapting UC-MSCs to standard culture conditions, possibly leading cells to increase the expression and secretion of these components.

These two proteomics screenings were then directly compared to further understand the similarities between low stiffness and oxygen priming (Figure 4C). Only three proteins were found to be upregulated by both experimental conditions, while six had inverse tendencies (Supplementary Figure 2E). Moreover, the twenty-five proteins identified to be commonly downregulated were described to be involved in ECM organization, corroborating the relevance of ECM for MSCs maintenance under standard culture conditions (Figure 4D and Supplementary Table 9).

Figure 4 – *Physiological priming decreases the secretion of ECM proteins.* The top 50 proteins (VIP>1, Supplementary Figure 2B) quantified with confidence on the three experimental groups: Standard (grey), Mechanomodulation (red) and Physioxia (yellow) are represented on the heatmap (with hierarchical clustering) (A) (protein names on Supplementary Table 8). The mechanomodulated secretome comprised 30 up-regulated (↑) proteins and 92 down-regulated (↓) proteins. Lowering the oxygen levels increased the secreted levels of 33 proteins and decreased the levels of 86 proteins. The significant biological processes (GO) of the filtered proteins (VIP>1, $p<0.05$, or both; $|Log_{1.5}FC|>1$) from each experimental condition are highlighted in B. No significant pathways were identified for proteins upregulated by mechanomodulation priming. Proteins altered in both low stiffness and oxygen levels were compared and further analyzed (C). The twenty-five common downregulated proteins are involved in ECM organization processes, according to the Reactome database (D; Supplementary Table 9). Abbreviations: Mechanomodulation (Mechano); Benjamini-Hochberg method (BH).

Expanding MSCs under standard culture conditions increases intra and extracellular levels of collagen and other ECM proteins

Next, to determine if the differences observed in the secretory profile of physiologically primed UC-MSCs were due to alterations in the cellular proteome (21), both screenings were compared separately for each experimental condition (Figure 5A-B and C-D, respectively). Priming UC-MSCs on soft platforms decreased the cellular levels of seventeen proteins, which was also reflected in secretome levels. These proteins were found to be involved in ECM organization and signal transduction (Figure 5B and Supplementary Table 10). Moreover, Zyxin and Laminin subunit gamma-1 appear to accumulate within the cell, while Apolipoprotein B-100 is highly secreted (Supplementary Figure 3A-B). Regarding the priming of UC-MSCs at physioxia environments, the results indicate that only three proteins present lower levels in both the intracellular and extracellular space: Fascin, Versican core protein, and Thrombospondin-2, proteins that are recognized to play a role on cell-matrix interactions (Figure 5D). Therefore, it can be concluded that UC-MSCs initiate

the readaptation to both physiological environments by modulating the extracellular space.

Figure 5 – *Intra and extracellular levels of ECM proteins decrease when MSCs initiate their readaptation to physiological environments.* For each primed method, proteins of interest previously selected for MSCs, cellular proteome, and secretome were compared. Venn diagrams represent common proteins shared by each cellular and secretome fraction for mechanomodulation and physioxia experimental conditions separately (A and C, respectively). Intersections were further explored. The seventeen proteins commonly downregulated proteins upon mechano-priming were analyzed using Reactome to identify significantly altered pathways (yellow) (B, Supplementary Table 10). Regarding physioxia-priming, three proteins were found to be decreased in both intracellular and extracellular spaces (F): Fascin (left), Versican core protein (middle) and Thrombospondin-2 (right) (Mann–Whitney; *p<0.05, **p<0.01).

Finally, to explore if the initial triggered pathways by the priming were kept during extended periods of cell culture, both time points were compared separately for each experimental condition (Figure 6A-B and C-E, respectively). Concerning the mechanical impact on UC-MSCs secretome, short periods increase the secretion of Peroxiredonin-5 (mitochondrial) and N-acetylglucosamine-6-sulfatase, but only the latter protein's levels are maintained for extended periods (Supplementary Figure 3C, top panel). In contrast, priming decreases the secretion of Endoplasmic reticulum chaperone BIP and Calumenin, whose levels are increased when UC-MSCs are readapted to physiological conditions (Supplementary Figure 3C, bottom panel). However, it appears that the rearrangement at the ECM is maintained over time, as well as PDGF and MET signaling (Figure 6B, Supplementary Table 11). Concerning the impact of time on physioxia-cultured UC-MSCs, cadherin-11 levels increased on physioxia-primed MSCs' secretome but decreased on readapted MSCs (Supplementary Figure 3D, top panel). Inversely, Tubulin alpha-1A chain, pappalysin-1, and carboxypeptidase A4 levels increased on the secretome of readapted to physioxia MSCs', but their protein levels were kept low during priming, compared to standard culture conditions, suggestive of a long-term regulation of the secretory profile of these proteins (Supplementary Figure 3D, bottom panel). Nevertheless, the upregulation of proteins associated with the immune system, metabolism of proteins, vesicle-mediated transport, and transport of small molecules pathways seem to be constant at both time points (Figure 6D, Supplementary Table 12), as well as the downregulation of ECM proteins (Figure 6E, Supplementary Table 13). Four of these proteins were shared by primed and UC-MSCs in response to adaptation for low stiffness and

oxygen levels, including collagen (Figure 6F). In conclusion, the results suggest that ECM proteins' levels decrease not only as a response to the initial readaptation of UC-MSCs to a physiological environment but are kept low for long periods, suggesting that they might be essential for maintaining the properties of these cells when expanded under low oxygen or stiffness environments.

Figure 6 – *Priming UC-MSCs initiates processes that are kept by readapted MSCs to physiological culture conditions.* Statistically different proteins selected for each experimental setup (mechanomodulation and physioxia for primed (48h) and readapted (7-10 days)) were compared (A and C, respectively). Intersections were further explored. The twenty-five proteins that have been downregulated in both periods have significant Reactome pathways (marked in yellow) (B, Supplementary Table 11). Concerning physioxia, the Reactome pathways associated with the common twenty up- and nineteen downregulated proteins are highlighted in yellow (D and E, respectively; Supplementary Tables 12 and 13). Common ECM proteins whose levels were decreased in the secretome by low stiffness or oxygen environments for both primed and readapted UC-MSCs are represented (except biglycan, for physioxia priming, which was not significant) (Mann-Whitney for priming experiments, comparing to the standard:*$p<0.05$, **$p<0.01$; t-test for readapted UC-MSCs, comparing to the respective standard: $^{\#}p<0.05$ (for mechanomodulation); $^{\$}p<0.05$, $^{\$\$}p<0.01$ (for physioxia).

Discussion

MSCs exhibit unique properties that allow them to modulate their surrounding environment by secreting molecules with immunomodulatory, antiapoptotic, or antioxidant properties (8, 10). Given the secretome's well-established beneficial characteristics and ready-to-use availability, there has been a focus on improving and modulating its composition. Published data suggests that reducing the stiffness and oxygen in the culture conditions of UC-MSCs to levels closer to those found in Wharton's jelly led to rearrangements in protein metabolism and translation processes (21). So, it has been hypothesized that the physiological cues could also alter the secretory profile of these cells.

The proteomic characterization of the CM of UC-MSCs cultured at 3kPa revealed differential secretion of several proteins (Figure 1A and B). Analysis of the biological processes associated with altered proteins indicated an upregulation of several protein disulfide isomerases (PDI) in the secretome (Supplementary Table 14). PDIs play a role in the redox folding within the endoplasmic reticulum (ER), ensuring the formation of disulfide bonds and, consequently, conformational changes in substrates (34). Notably, increased PDI expression has been associated with promoting cell survival in hindlimb ischemia damage, suggesting a putative therapeutic advantage (35). This

finding and the higher secretion of antioxidant proteins may be pivotal in modulating the harsh environment typically encountered by UC-MSCs at the injury site (Figure 1C, F). Furthermore, the identification of proteins involved in the TCA cycle and other mitochondrial-specific proteins suggests a possible increase in mitochondrial transfer, a process recognized for its importance in restoring oxidative phosphorylation (36, 37). Mitochondrial activity has previously been shown described to be influenced by matrix stiffness and physioxia, playing a crucial role in the differentiation processes of MSCs by balancing ROS levels and controlling gene expression (38-41). Therefore, future studies should involve a more comprehensive characterization of mitochondria proteins present in the secretome, encompassing their activity and morphology.

Additionally, a decrease in several 40s ribosomal subunits, known for their involvement in translation and rRNA processing mechanisms, was observed in the secretome (Figure 1C, E). The presence of ribosomes in the extracellular environment has already been documented for other cell types (42). The role of ribosomal proteins and RNA composition in regulating gene expression has gained attention in the past few years (43, 44). Hence, exploring the differential secretion of these structures by UC-MSCs and mitochondrial proteins could be a promising approach to investigate the potential implications on the cell signaling mechanisms triggered at the lesion site.

Moreover, culturing UC-MSCs at physioxia deeply altered the secretory profile of these cells for both long and short periods (Figure 2A, B, and Figure 4A). Proteins associated with immunomodulatory processes (both innate and adaptative), particularly immunoglobulins and fibrinolysis, were found to be increased in the CM (Supplementary Tables 3, 5, and 14). In fact, previous studies have shown that exposing MSCs to low levels of oxygen enhances their immunomodulatory properties (45). Conversely, proteins associated with cell adhesion, angiogenesis, or ossification were found to be downregulated. Notably, many of these proteins are ECM components, including collagen, fibronectin, and laminin (Supplementary Table 15). These proteins play a role in determining stem cell fate, suggesting that standard culture conditions may upregulate their secretion and possibly bias their naïve therapeutical properties (46).

Reduced stiffness and oxygen levels decreased ECM protein secretion (Figure 3B and 5B,D). So, to further investigate the commonly modulated secreted proteins, both screenings were compared (Figure 6A,C). The results revealed that collagen was the major component altered (Figure 3B, Figure 6B, E, F; Supplementary Table 16). Collagen fibril crosslinking, which depends on posttranslational modifications, influences tissue tensile strength (47). Higher collagen composition is typically associated with increased tissue elastic modulus, potentially leading to an osteogenic commitment of MSCs (48). Hence, it is intriguing to note that MSCs cultured under physioxia conditions can possibly modulate the stiffness of their microenvironment, which has implications for their cell fate. However, further studies are necessary to analyze the 3D organization of the secreted collagen fibrils since peroxidasin homolog, involved in collagen crosslinking, was also found to be decreased (49). Other matrix constituents, such as fribrilin-1 (P35555) and biglycan (P21810) (Figure 6F), known to determine stem cell fate, were also downregulated (50, 51). In fact, the results suggest that the reorganization of the extracellular space is a key factor in the adaptation of MSCs to standard culture conditions since the differential expression of these components is observed upon priming (48h), particularly in response to mechanical cues (Figure 4B, 5B). Therefore, future work should focus on studying the mechanisms by which alterations in ECM composition affect signaling pathways and their impact on MSC differentiation and therapeutic efficacy. The remodeling of ECM proteins can significantly impact receptor tyrosine kinase signaling pathways, including those mediated by PDGF (Supplementary Tables 10 and 12). Collagen has been shown to target Discoidin domain receptor 1, a collagen-activated receptor tyrosine kinase, thereby modulating cell morphology, ERK activation, and osteogenic commitment (52). Other works have also described the PDGF pathway as being crucial for MSCs' growth and proliferation (53, 54). Specifically, by interacting with integrins, ECM components can interfere with the PI3K/AKT pathway and alter stem cell fate (Figure 3F) (55). Nevertheless, future research should validate how ECM rearrangements differentially activate these pathways.

The changes in the CM composition induced by the modulation of MSCs' culture conditions may influence the regenerative potential of the secretome, depending on the target tissue. For instance, a decrease in the levels of ECM

proteins essential to promote bone regeneration, such as proteoglycans or C-type lectin (Supplementary Tables 1, 4, and 14), might make the application of physiologically modulated secretome more suitable to other organ systems rather than the skeletal system (56, 57). In addition to common features, a subset of proteins linked to the calnexin/calreticulin cycle (part of the ER chaperon system) were found to be inversely modulated by low stiffness and oxygen levels. These proteins include calreticulin, neutral alpha-glucosidase AB, and protein disulfide-isomerase A3 (Supplementary Figure 1G, Supplementary Table 17). Calreticulin plays a crucial role in mediating osteogenesis, cell adhesion, and fibrotic processes by stimulating fibronectin and collagen deposition in other cell types (58-61). However, the present study suggests that other pathways might also be interfering with ECM deposition since several collagen fibrils were found to be decreased on soft substrates.

In conclusion, analysis of the CM revealed that expanding UC-MSCs under high stiffness and hyperoxia environments (typical of standard culture conditions) may compromise the secretion of PDIs and mitochondrial proteins, as well as proteins involved in immune responses, key players for cell survival at the site of injury. In addition, replicating Wharton's Jelly stiffness and oxygen levels led to the downregulation of several ECM components. This suggests that maintaining UC-MSCs in an artificial environment might be upregulating these components, biasing stem cell fate, and potentially affecting the therapeutical properties of the secretome.

List of Abbreviations

CM – Conditioned medium

DDA – Data Dependent Acquisition

DIA – Data Independent Acquisition

ECM – Extracellular matrix

ER – Endoplasmic reticulum

FDR – False Discovery Rate

GO – Gene Ontology

MET - Hepatocyte growth factor receptor

MSCs – Mesenchymal stem cells

PDGF - Platelet-Derived Growth Factor

PDI - Protein disulfide isomerase

PDMS – Polydimethylsiloxane

PLS-DA - Partial Least-Squares Discriminant Analysis

ROS – Reactive oxygen species

SWATH - Sequential Window Acquisition of all Theoretical Mass Spectra

TCA - Tricarboxylic acid cycle

UC – Umbilical cord

UC-MSCs – Umbilical cord mesenchymal stem cells

References

1. Merimi M, El-Majzoub R, Lagneaux L, Moussa Agha D, Bouhtit F, Meuleman N, Fahmi H, Lewalle P, Fayyad-Kazan M, Najar M. The Therapeutic Potential of Mesenchymal Stromal Cells for Regenerative Medicine: Current Knowledge and Future Understandings. Frontiers in Cell and Developmental Biology. 2021;9.
2. Han Y, Li X, Zhang Y, Han Y, Chang F, Ding J. Mesenchymal Stem Cells for Regenerative Medicine. Cells. 2019;8(8):886.
3. Dominici M, Le Blanc K, Mueller I, Slaper-Cortenbach I, Marini F, Krause D, Deans R, Keating A, Prockop D, Horwitz E. Minimal criteria for defining multipotent mesenchymal stromal cells. The International Society for Cellular Therapy position statement. Cytotherapy. 2006;8(4):315-7.
4. Foo JB, Looi QH, Chong PP, Hassan NH, Yeo GEC, Ng CY, Koh B, How CW, Lee SH, Law JX. Comparing the Therapeutic Potential of Stem Cells and their Secretory Products in Regenerative Medicine. Stem Cells Int. 2021;2021:2616807.
5. Comella K, Parlo M, Daly R, Depasquale V, Edgerton E, Mallory P, Schmidt R, Drake WP. Safety Analysis of Autologous Stem Cell Therapy in a Variety of Degenerative Diseases and Injuries Using the Stromal Vascular Fraction. J Clin Med Res. 2017;9(11):935-42.
6. Liang J, Zhang H, Zhao C, Wang D, Ma X, Zhao S, Wang S, Niu L, Sun L. Effects of allogeneic mesenchymal stem cell transplantation in the treatment of liver cirrhosis caused by autoimmune diseases. Int J Rheum Dis. 2017;20(9):1219-26.
7. Hmadcha A, Martin-Montalvo A, Gauthier BR, Soria B, Capilla-Gonzalez V. Therapeutic Potential of Mesenchymal Stem Cells for Cancer Therapy. Front Bioeng Biotechnol. 2020;8:43.
8. Pinho AG, Cibrão JR, Silva NA, Monteiro S, Salgado AJ. Cell Secretome: Basic Insights and Therapeutic Opportunities for CNS Disorders. Pharmaceuticals (Basel). 2020;13(2).
9. Műzes G, Sipos F. Mesenchymal Stem Cell-Derived Secretome: A Potential Therapeutic Option for Autoimmune and Immune-Mediated Inflammatory Diseases. Cells. 2022;11(15).

10. González-González A, García-Sánchez D, Dotta M, Rodríguez-Rey JC, Pérez-Campo FM. Mesenchymal stem cells secretome: The cornerstone of cell-free regenerative medicine. World J Stem Cells. 2020;12(12):1529-52.
11. Vizoso FJ, Eiro N, Cid S, Schneider J, Perez-Fernandez R. Mesenchymal Stem Cell Secretome: Toward Cell-Free Therapeutic Strategies in Regenerative Medicine. Int J Mol Sci. 2017;18(9).
12. Daneshmandi L, Shah S, Jafari T, Bhattacharjee M, Momah D, Saveh-Shemshaki N, Lo KW, Laurencin CT. Emergence of the Stem Cell Secretome in Regenerative Engineering. Trends Biotechnol. 2020;38(12):1373-84.
13. Pires AO, Mendes-Pinheiro B, Teixeira FG, Anjo SI, Ribeiro-Samy S, Gomes ED, Serra SC, Silva NA, Manadas B, Sousa N, Salgado AJ. Unveiling the Differences of Secretome of Human Bone Marrow Mesenchymal Stem Cells, Adipose Tissue-Derived Stem Cells, and Human Umbilical Cord Perivascular Cells: A Proteomic Analysis. Stem Cells Dev. 2016;25(14):1073-83.
14. Chouaib B, Haack-Sørensen M, Chaubron F, Cuisinier F, Collart-Dutilleul PY. Towards the Standardization of Mesenchymal Stem Cell Secretome-Derived Product Manufacturing for Tissue Regeneration. Int J Mol Sci. 2023;24(16).
15. Noronha NdC, Mizukami A, Caliári-Oliveira C, Cominal JG, Rocha JLM, Covas DT, Swiech K, Malmegrim KCR. Priming approaches to improve the efficacy of mesenchymal stromal cell-based therapies. Stem Cell Research & Therapy. 2019;10(1):131.
16. Wechsler ME, Rao VV, Borelli AN, Anseth KS. Engineering the MSC Secretome: A Hydrogel Focused Approach. Adv Healthc Mater. 2021;10(7):e2001948.
17. Wang JHC, Thampatty BP. Chapter 7 Mechanobiology of Adult and Stem Cells. International Review of Cell and Molecular Biology. 271: Academic Press; 2008. p. 301-46.
18. Mohyeldin A, Garzón-Muvdi T, Quiñones-Hinojosa A. Oxygen in Stem Cell Biology: A Critical Component of the Stem Cell Niche. Cell Stem Cell. 2010;7(2):150-61.
19. Gervaso F, Boschetti F, Pennati G. Evaluation of the Wharton's jelly poroelastic parameters through compressive tests on placental and foetal ends of human umbilical cords. J Mech Behav Biomed Mater. 2014;35:51-8.
20. Keeley TP, Mann GE. Defining Physiological Normoxia for Improved Translation of Cell Physiology to Animal Models and Humans. Physiological Reviews. 2018;99(1):161-234.
21. Caramelo I, Mendes VM, Domingues C, Anjo SI, Geraldo M, Cardoso CMP, Grãos M, Manadas B. Mimicking physiological stiffness or oxygen levels in vitro reorganizes mesenchymal stem cells machinery toward a more naïve phenotype. 2024(submitted).
22. Domingues C, Geraldo AM, Anjo SI, Matos A, Almeida C, Caramelo I, Lopes-da-Silva JA, Paiva A, Carvalho J, Pires das Neves R, Manadas B, Grãos M. Cofilin-1 Is a Mechanosensitive Regulator of Transcription. Frontiers in Cell and Developmental Biology. 2020;8.
23. Caramelo I, Anjo SI, Mendes VM, Grãos M, Manadas B. Non-targeted proteomics profiling of mesenchymal stem cells' secretome. In: Springer, editor. Mesenchymal stem cells2024(submited).
24. Anjo SI, Simões I, Castanheira P, Grãos M, Manadas B. Use of recombinant proteins as a simple and robust normalization method for untargeted proteomics screening: exhaustive performance assessment. Talanta. 2019;205:120163.

25. Anjo SI, Santa C, Manadas B. Short GeLC-SWATH: a fast and reliable quantitative approach for proteomic screenings. Proteomics. 2015;15(4):757-62.
26. Manadas B, Santos AR, Szabadfi K, Gomes JR, Garbis SD, Fountoulakis M, Duarte CB. BDNF-induced changes in the expression of the translation machinery in hippocampal neurons: protein levels and dendritic mRNA. J Proteome Res. 2009;8(10):4536-52.
27. Shin J, Kwon Y, Lee S, Na S, Hong EY, Ju S, Jung H-G, Kaushal P, Shin S, Back JH, Choi SY, Kim EH, Lee SJ, Park YE, Ahn H-S, Ahn Y, Kabir MH, Park S-J, Yang WS, Yeom J, Bang OY, Ha C-W, Lee J-W, Kang U-B, Kim H-J, Park K-S, Lee JE, Lee JE, Kim JY, Kim KP, Kim Y, Hirano H, Yi EC, Cho J-Y, Paek E, Lee C. Common Repository of FBS Proteins (cRFP) To Be Added to a Search Database for Mass Spectrometric Analysis of Cell Secretome. Journal of Proteome Research. 2019;18(10):3800-6.
28. Pang Z, Chong J, Zhou G, de Lima Morais DA, Chang L, Barrette M, Gauthier C, Jacques P-É, Li S, Xia J. MetaboAnalyst 5.0: narrowing the gap between raw spectra and functional insights. Nucleic Acids Research. 2021;49(W1):W388-W96.
29. Fonseka P, Pathan M, Chitti SV, Kang T, Mathivanan S. FunRich enables enrichment analysis of OMICs datasets. J Mol Biol. 2021;433(11):166747.
30. Gillespie M, Jassal B, Stephan R, Milacic M, Rothfels K, Senff-Ribeiro A, Griss J, Sevilla C, Matthews L, Gong C, Deng C, Varusai T, Ragueneau E, Haider Y, May B, Shamovsky V, Weiser J, Brunson T, Sanati N, Beckman L, Shao X, Fabregat A, Sidiropoulos K, Murillo J, Viteri G, Cook J, Shorser S, Bader G, Demir E, Sander C, Haw R, Wu G, Stein L, Hermjakob H, D'Eustachio P. The reactome pathway knowledgebase 2022. Nucleic Acids Research. 2021;50(D1):D687-D92.
31. Kanehisa M, Furumichi M, Sato Y, Kawashima M, Ishiguro-Watanabe M. KEGG for taxonomy-based analysis of pathways and genomes. Nucleic Acids Res. 2023;51(D1):D587-d92.
32. Hulsen T, de Vlieg J, Alkema W. BioVenn – a web application for the comparison and visualization of biological lists using area-proportional Venn diagrams. BMC Genomics. 2008;9(1):488.
33. Caramelo I, Mendes VM, Domingues C, Anjo SI, Geraldo M, Cardoso CMP, Grãos M, Manadas B. Mimicking physiological stiffness or oxygen levels in vitro reorganizes mesenchymal stem cells machinery toward a more naïve phenotype. bioRxiv. 2024:2024.06.11.598426.
34. Medinas DB, Rozas P, Hetz C. Critical roles of protein disulfide isomerases in balancing proteostasis in the nervous system. J Biol Chem. 2022;298(7):102087.
35. Di Rocco G, Baldari S, Gentile A, Capogrossi M, Toietta G. Protein disulfide isomerase as a prosurvival factor in cell therapy for muscular and vascular diseases. Stem Cell Research & Therapy. 2018;9(1):250.
36. Gomzikova MO, James V, Rizvanov AA. Mitochondria Donation by Mesenchymal Stem Cells: Current Understanding and Mitochondria Transplantation Strategies. Front Cell Dev Biol. 2021;9:653322.
37. Mohammadalipour A, Dumbali SP, Wenzel PL. Mitochondrial Transfer and Regulators of Mesenchymal Stromal Cell Function and Therapeutic Efficacy. Front Cell Dev Biol. 2020;8:603292.
38. Ma S, Ding R, Cao J, Liu Z, Li A, Pei D. Mitochondria transfer reverses the inhibitory effects of low stiffness on osteogenic differentiation of human mesenchymal stem cells. European Journal of Cell Biology. 2023;102(2):151297.

39. Li Q, Gao Z, Chen Y, Guan M-X. The role of mitochondria in osteogenic, adipogenic and chondrogenic differentiation of mesenchymal stem cells. Protein & Cell. 2017;8(6):439-45.
40. Ejtehadifar M, Shamsasenjan K, Movassaghpour A, Akbarzadehlaleh P, Dehdilani N, Abbasi P, Molaeipour Z, Saleh M. The Effect of Hypoxia on Mesenchymal Stem Cell Biology. Adv Pharm Bull. 2015;5(2):141-9.
41. Lavrentieva A, Majore I, Kasper C, Hass R. Effects of hypoxic culture conditions on umbilical cord-derived human mesenchymal stem cells. Cell Commun Signal. 2010;8:18.
42. Tosar JP, Segovia M, Castellano M, Gámbaro F, Akiyama Y, Fagúndez P, Olivera Á, Costa B, Possi T, Hill M, Ivanov P, Cayota A. Fragmentation of extracellular ribosomes and tRNAs shapes the extracellular RNAome. Nucleic Acids Research. 2020;48(22):12874-88.
43. Gingold H, Tehler D, Christoffersen Nanna R, Nielsen Morten M, Asmar F, Kooistra Susanne M, Christophersen Nicolaj S, Christensen LL, Borre M, Sørensen Karina D, Andersen Lars D, Andersen Claus L, Hulleman E, Wurdinger T, Ralfkiær E, Helin K, Grønbæk K, Ørntoft T, Waszak Sebastian M, Dahan O, Pedersen Jakob S, Lund Anders H, Pilpel Y. A Dual Program for Translation Regulation in Cellular Proliferation and Differentiation. Cell. 2014;158(6):1281-92.
44. Han Z, Zhang Q, Zhu Y, Chen J, Li W. Ribosomes: An Exciting Avenue in Stem Cell Research. Stem Cells Int. 2020;2020:8863539.
45. Su Y, Xu C, Cheng W, Zhao Y, Sui L, Zhao Y. Pretreated Mesenchymal Stem Cells and Their Secretome: Enhanced Immunotherapeutic Strategies. Int J Mol Sci. 2023;24(2).
46. Gattazzo F, Urciuolo A, Bonaldo P. Extracellular matrix: A dynamic microenvironment for stem cell niche. Biochimica et Biophysica Acta (BBA) - General Subjects. 2014;1840(8):2506-19.
47. Muncie JM, Weaver VM. The Physical and Biochemical Properties of the Extracellular Matrix Regulate Cell Fate. Curr Top Dev Biol. 2018;130:1-37.
48. Smith LR, Cho S, Discher DE. Stem Cell Differentiation is Regulated by Extracellular Matrix Mechanics. Physiology. 2018;33(1):16-25.
49. Lee SW, Kim HK, Naidansuren P, Ham KA, Choi HS, Ahn HY, Kim M, Kang DH, Kang SW, Joe YA. Peroxidasin is essential for endothelial cell survival and growth signaling by sulfilimine crosslink-dependent matrix assembly. Faseb j. 2020;34(8):10228-41.
50. Smaldone S, Clayton NP, del Solar M, Pascual G, Cheng SH, Wentworth BM, Schaffler MB, Ramirez F. Fibrillin-1 Regulates Skeletal Stem Cell Differentiation by Modulating TGFβ Activity Within the Marrow Niche. J Bone Miner Res. 2016;31(1):86-97.
51. Wu B, Ma X, Zhu D, Liu Y, Sun Z, Liu S, Xue B, Du M, Yin X. Lentiviral delivery of biglycan promotes proliferation and increases osteogenic potential of bone marrow-derived mesenchymal stem cells in vitro. J Mol Histol. 2013;44(4):423-31.
52. Lund AW, Stegemann JP, Plopper GE. Mesenchymal Stem Cells Sense Three Dimensional Type I Collagen through Discoidin Domain Receptor 1. Open Stem Cell J. 2009;1:40-53.
53. Ng F, Boucher S, Koh S, Sastry KSR, Chase L, Lakshmipathy U, Choong C, Yang Z, Vemuri MC, Rao MS, Tanavde V. PDGF, TGF-β, and FGF signaling is important for

differentiation and growth of mesenchymal stem cells (MSCs): transcriptional profiling can identify markers and signaling pathways important in differentiation of MSCs into adipogenic, chondrogenic, and osteogenic lineages. Blood. 2008;112(2):295-307.
54. Sun Z, Fukui M, Taketani S, Kako A, Kunieda S, Kakudo N. Predominant control of PDGF/PDGF receptor signaling in the migration and proliferation of human adipose derived stem cells under culture conditions with a combination of growth factors. Exp Ther Med. 2024;27(4):156.
55. Ramazzotti G, Ratti S, Fiume R, Follo MY, Billi AM, Rusciano I, Owusu Obeng E, Manzoli L, Cocco L, Faenza I. Phosphoinositide 3 Kinase Signaling in Human Stem Cells from Reprogramming to Differentiation: A Tale in Cytoplasmic and Nuclear Compartments. Int J Mol Sci. 2019;20(8).
56. Yue R, Shen B, Morrison SJ. Clec11a/osteolectin is an osteogenic growth factor that promotes the maintenance of the adult skeleton. Elife. 2016;5.
57. Chen J, Sun T, You Y, Wu B, Wang X, Wu J. Proteoglycans and Glycosaminoglycans in Stem Cell Homeostasis and Bone Tissue Regeneration. Frontiers in Cell and Developmental Biology. 2021;9.
58. Van Duyn Graham L, Sweetwyne MT, Pallero MA, Murphy-Ullrich JE. Intracellular Calreticulin Regulates Multiple Steps in Fibrillar Collagen Expression, Trafficking, and Processing into the Extracellular Matrix*. Journal of Biological Chemistry. 2010;285(10):7067-78.
59. Pandya UM, Manzanares MA, Tellechea A, Egbuta C, Daubriac J, Jimenez-Jaramillo C, Samra F, Fredston-Hermann A, Saadipour K, Gold LI. Calreticulin exploits TGF-β for extracellular matrix induction engineering a tissue regenerative process. The FASEB Journal. 2020;34(12):15849-74.
60. Alvandi Z, Al-Mansoori LJR, Opas M. Calreticulin regulates Src kinase in osteogenic differentiation from embryonic stem cells. Stem Cell Research. 2020;48:101972.
61. Gold LI, Eggleton P, Sweetwyne MT, Van Duyn LB, Greives MR, Naylor SM, Michalak M, Murphy-Ullrich JE. Calreticulin: non-endoplasmic reticulum functions in physiology and disease. Faseb j. 2010;24(3):665-83.

Supplementary figures

Supplementary Figure 1 – *Readaptation of UC-MSCs to physiological conditions differentially modulate intra and extracellular levels of the proteins.* For mechanomodulated UC-MSCs, six proteins increased in the secretome but with lower levels on the cellular fraction (A), while four proteins were less secreted but increased levels on the cellular fraction (B) (t-test; *p<0.05). Considering physioxia-adapted UC-MSCs, the protein whose levels are higher in the secretome compared to the cellular proteome, or the three proteins that appear to accumulate within the cells are represented in the Violin plots (C and D, respectively) (t-test; *p<0.05). Comparing both experimental conditions, it was possible to identify ATP synthase subunit alpha (E), whose levels are increased in both systems and Talin-1 (F), which is increased in physioxia and decreased by low stiffness conditions (t-test, *p<0.05). According to the Kegg Pathway database, proteins with opposite tendencies in physiological environments might be involved in the calnexin/calreticulin cycle (G). In detail, the mapped proteins are highlighted in circles (grey: proteins that belong to the pathway; dark green: upregulated on mechanomodulation; light brown: downregulated on physioxia). Abbreviations: SRP: signal recognition particle; BiP: Binding immunoglobulin protein; GlcI: mannosyl-oligosaccharide glucosidase; GlcII: glucosidase II alpha subunit; CNX: calnexin; ERP57: protein disulfide-isomerase A3; CRT: Calreticulin; ERManI: mannosidase alpha class 1A member 2; UUGT: UDP-glucose glycoprotein glucosyltransferase 2.

Supplementary Figure 2 – *Composition of MSCs secretome is differentially altered by mechanomodulation or physioxia priming.* A PCA and a PLS-DA model were generated using all 413 quantified proteins in the three experimental groups (standard (grey), mechano (orange), physioxia (red)) (A, B respectively). Also, the PLS-DA scores plot illustrates mechanomodulation and physioxia priming individually, compared to the standard condition (C, left and right, respectively). Cellular components (GO) of significant proteins (VIP>1, $p<0.05$, or both; $|Log_{1.5}FC|>1$) are represented in D. Violin plots represent proteins with inverse tendencies on both experimental conditions (top and bottom) and common upregulated proteins (middle) (E). (Kruskal-Wallis test; *$p<0.05$, **$p<0.01$)

Supplementary Figure 3 – *The initial secretory pattern of UC-MSCs is altered during their readaptation to physiological environments.* In response to mechanomodulation priming, two proteins appear to accumulate in the intracellular space (A) and the one that appears to be translocated to the extracellular space in MSCs primed by mechanomodulation (B) (Mann–Whitney test; **$p<0.01$). Primed and readapted UC-MSCs secretome were then compared for each experimental condition. Lowering stiffness for extended periods leads to the upregulation of peroxiredoxin-5 (mitochondrial) and N-acetylglucosamine-6-sulfatase, but the levels of the former were decreased in long-term cultures (C, top panel). Also, two proteins were decreased by mechano-priming, but their levels in the secretome increased for readapted UC-MSCs: endoplasmic reticulum chaperone BIP and calumenin (C, bottom panel) (Mann-Whitney for priming; t-test for readapted MSCs; *$p<0.05$). Concerning physioxia, Cadherin-11 levels were increased upon priming but decreased after extended periods under physiological oxygen levels (D, top panel). In contrast, three proteins (Tubulin alpha-1A chain, Pappalysin-1 and Carboxypeptidase A4) expression was increased on the long-term experimental setup but decreased on priming (D, bottom panel) (Mann-Whitney for priming; t-test for readapted MSCs; *$p<0.05$, **$p<0.01$). The total intensity of the secretome was not altered by the experimental conditions (E).

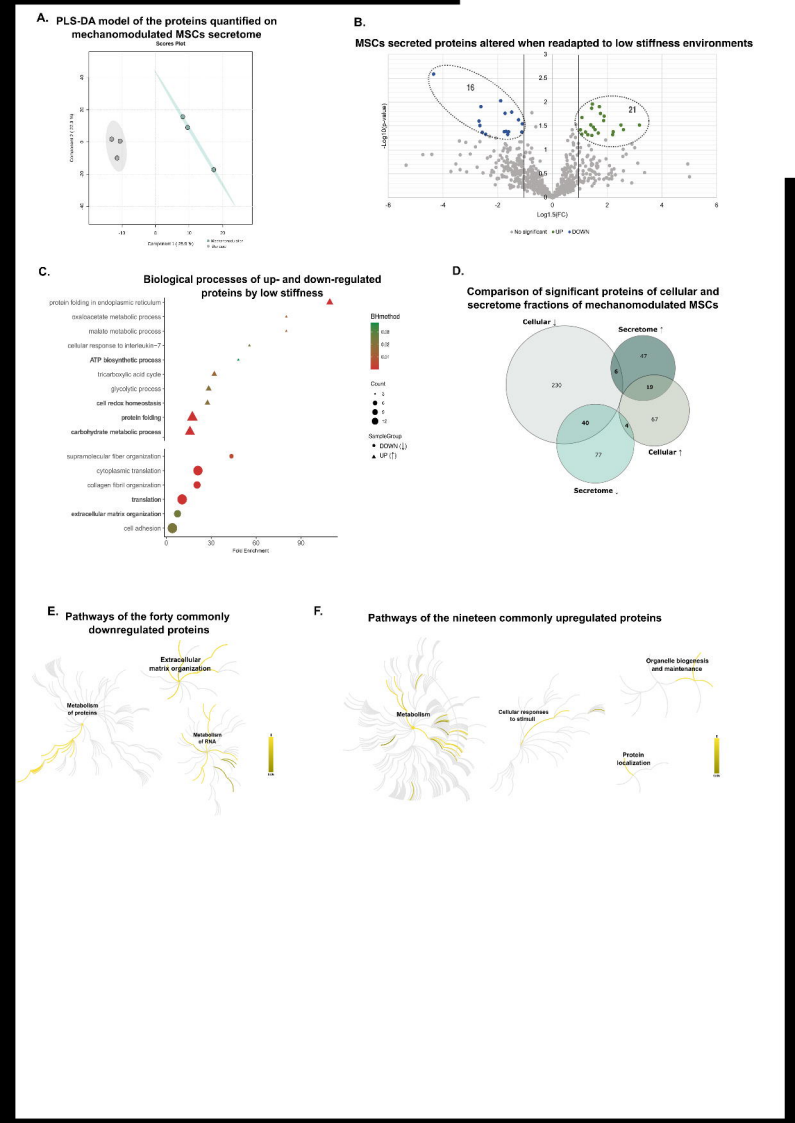
A.
PLS-DA model of the proteins quantified on mechanomodulated MSCs secretome
Scores Plot
B.
MSCs secreted proteins altered when readapted to low stiffness environments
16
21
-Log10(p-value)
Log1.5(FC)
No significant
UP
DOWN
C.
Biological processes of up- and down-regulated proteins by low stiffness
protein folding in endoplasmic reticulum
oxaloacetate metabolic process
malate metabolic process
cellular response to interleukin-7
ATP biosynthetic process
tricarboxylic acid cycle
glycolytic process
cell redox homeostasis
protein folding
carbohydrate metabolic process
supramolecular fiber organization
cytoplasmic translation
collagen fibril organization
translation
extracellular matrix organization
cell adhesion
BHmethod
Count
SampleGroup
DOWN (↓)
UP (↑)
Fold Enrichment
D.
Comparison of significant proteins of cellular and secretome fractions of mechanomodulated MSCs
Cellular ↓
Secretome ↑
Cellular ↑
Secretome ↓
230
47
6
19
67
40
4
77
E.
Pathways of the forty commonly downregulated proteins
Extracellular matrix organization
Metabolism of proteins
Metabolism of RNA
F.
Pathways of the nineteen commonly upregulated proteins
Organelle biogenesis and maintenance
Metabolism
Cellular responses to stimuli
Protein localization

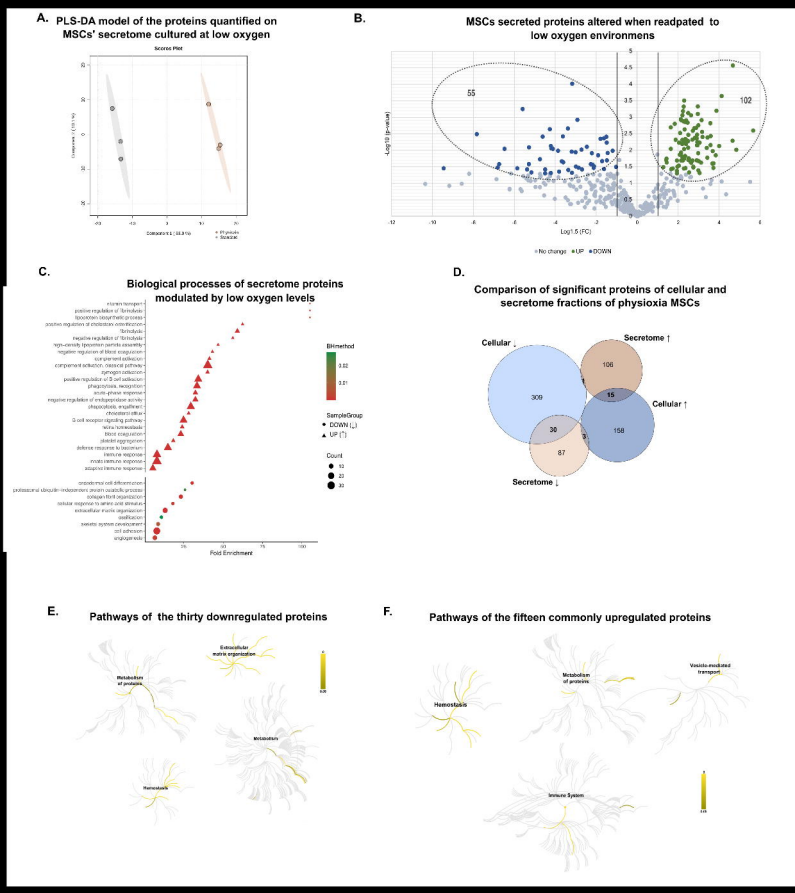
A.
PLS-DA model of the proteins quantified on MSCs' secretome cultured at low oxygen
Scores Plot
Component 1 (58.3 %)
Component 2 (10.1 %)
Pt proteins
Standard
B.
MSCs secreted proteins altered when readpated to low oxygen environmens
55
102
-Log10 (p-value)
Log1.5 (FC)
No change
UP
DOWN
C.
Biological processes of secretome proteins modulated by low oxygen levels
Biomethod
3.82
3.21
SampleGroup
DOWN (↓)
UP (↑)
Count
10
20
30
Fold Enrichment
D.
Comparison of significant proteins of cellular and secretome fractions of physioxia MSCs
Cellular ↓
Secretome ↑
Cellular ↑
Secretome ↓
106
15
309
158
30
87
E.
Pathways of the thirty downregulated proteins
Extracellular matrix organization
Metabolism of proteins
Metabolism
Hemostasis
F.
Pathways of the fifteen commonly upregulated proteins
Metabolism of proteins
Vesicle-mediated transport
Hemostasis
Immune System

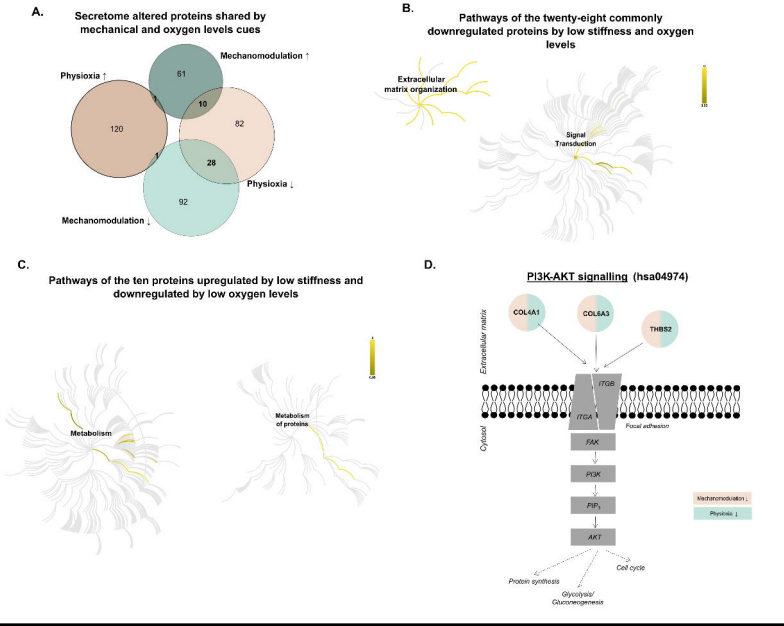
A.
Secretome altered proteins shared by mechanical and oxygen levels cues
Mechanomodulation ↑
Physioxia ↑
Physioxia ↓
Mechanomodulation ↓
61
1
10
120
82
1
28
92
B.
Pathways of the twenty-eight commonly downregulated proteins by low stiffness and oxygen levels
Extracellular matrix organization
Signal Transduction
C.
Pathways of the ten proteins upregulated by low stiffness and downregulated by low oxygen levels
Metabolism
Metabolism of proteins
D.
PI3K-AKT signalling (hsa04974)
Extracellular matrix
COL4A1
COL6A3
THBS2
ITGB
ITGA
Focal adhesion
Cytosol
FAK
PI3K
PIP3
AKT
Mechanomodulation ↓
Physioxia ↓
Cell cycle
Protein synthesis
Glycolysis/ Gluconeogenesis

A.
Heatmap of the TOP 50 secreted proteins altered upon physiological priming
Mechano
Physioxia
Standard
B.
Biological processes of secreted proteins altered upon priming
negative regulation of endopeptidase activity
reverse cholesterol transport
high-density lipoprotein particle remodeling
extracellular matrix organization
collagen fibril organization
positive regulation of cell death
complement activation, classical pathway
vasodilation
positive regulation of phospholipid efflux
lipoprotein biosynthetic process
cholesterol efflux
fibrinolysis
high-density lipoprotein particle assembly
positive regulation of cholesterol esterification
high-density lipoprotein particle clearance
immune response
adaptive immune response
protein targeting
cellular response to interleukin-7
viral entry into host cell
meiotic cytokinesis
meiotic chromosome movement towards spindle pole
protein folding in endoplasmic reticulum
protein folding
collagen catabolic process
cellular protein metabolic process
glycolytic process
proteolysis
response to mechanical stimulus
positive regulation of receptor-mediated endocytosis
wound healing
ventral trunk neural crest cell migration
tendon development
sympathetic neuron projection guidance
sympathetic neuron projection extension
semaphorin-plexin signaling pathway involved in neuron projection guidance
regulation of amyloid-beta clearance
positive regulation of smooth muscle cell migration
positive regulation of amyloid fibril formation
negative regulation of transforming growth factor beta production
negative regulation of angiogenesis
negative regulation by host of viral process
gonadotrophin-releasing hormone neuronal migration to the hypothalamus
sensory neuron axon guidance
positive regulation of substrate-dependent cell migration
cell attachment to substrate
facioacoustic ganglion development
eye morphogenesis
animal organ morphogenesis
negative regulation of amyloid fibril formation
heparan sulfate proteoglycan biosynthetic process
vestibulocochlear nerve structural organization
positive regulation of neurofibrillary tangle assembly
negative regulation of glycoprotein metabolic process
negative regulation of exo-alpha-sialidase activity
negative regulation of endodermal cell differentiation
negative regulation by host of viral glycoprotein metabolic activity
negative regulation by host of viral exo-alpha-sialidase process
dorsal root ganglion morphogenesis
collagen-activated tyrosine kinase receptor signaling pathway
cellular response to amino acid stimulus
angiogenesis
neural crest cell migration involved in autonomic nervous system development
skin development
tissue development
basement membrane organization
sequestering of TGFbeta in extracellular matrix
supramolecular fiber organization
skeletal system development
negative regulation of blood coagulation
ossification
cell-matrix adhesion
endodermal cell differentiation
cell adhesion
Mechano ↓
Physioxia ↓
Physioxia ↑
p-value (BHmethod)
0.04
0.03
0.02
0.01
Count
5
10
15
20
C.
Common secreted proteins upon physiological priming
Physioxia ↓
59
25
2
Mechano ↑
25
63
4
3
26
Mechano ↓
Physioxia ↑
D.
Pathways of common twenty five downregulated proteins
Collagen degradation
Collagen chain trimerization
Crosslinking of collagen fibrils
Degradation of the ECM
ECM proteoglycans
Collagen formation
Elastic fiber formation
Non-integrin membrance ECM interactions
Anchoring fibril formation
Integrin and cell surface interaction
0
0.05
Extracellular matrix organization

A.

Common altered proteins on the secretome and cellular proteome of mechanomodulated-primed MSCs

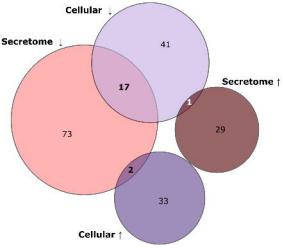

B.

Significant pathways of the seventeed proteins with lower abundance on both the secretome and cellular proteome of mechano-primed MSCs

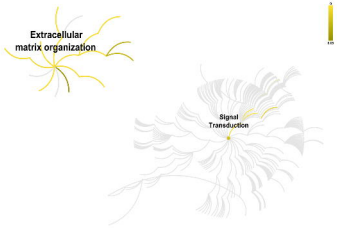

C.

Common altered proteins on the secretome and cellular proteome of physioxia-primed MSCs

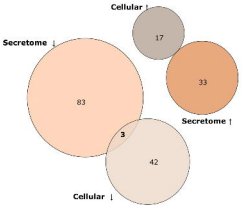

D.

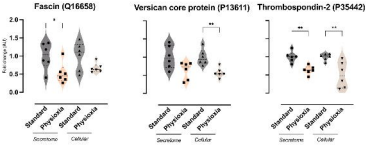

Common altered proteins on the secretome of primed- and readapted mechanomodulated MSCs

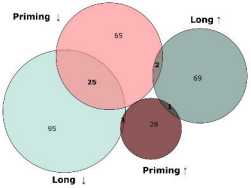

C. Common altered proteins on the secretome of primed- and readapted to physiological oxygen MSCs

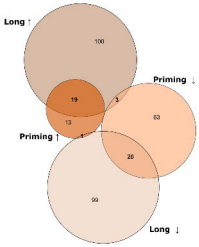

B. Pathways of common twenty five proteins modulated by priming and long exposure to low stiffness conditions

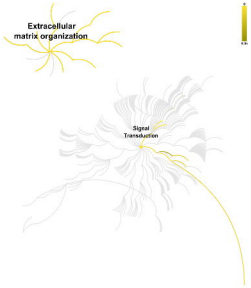

D. Pathways of common nineteen upregulated proteins by long exposure and priming under low oxygen levels

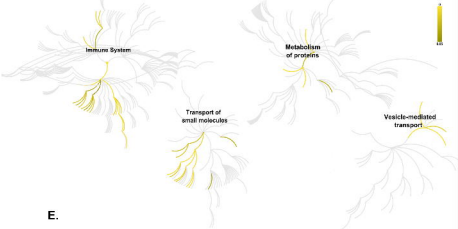

E. Pathways of common twenty downregulated proteins by long exposure and priming under low oxygen levels

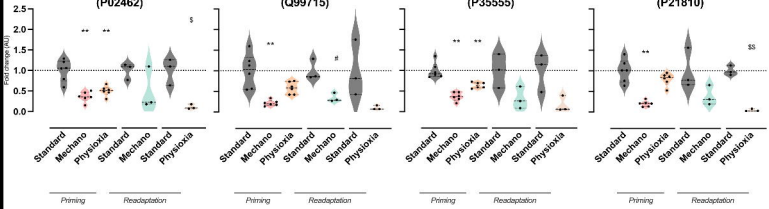

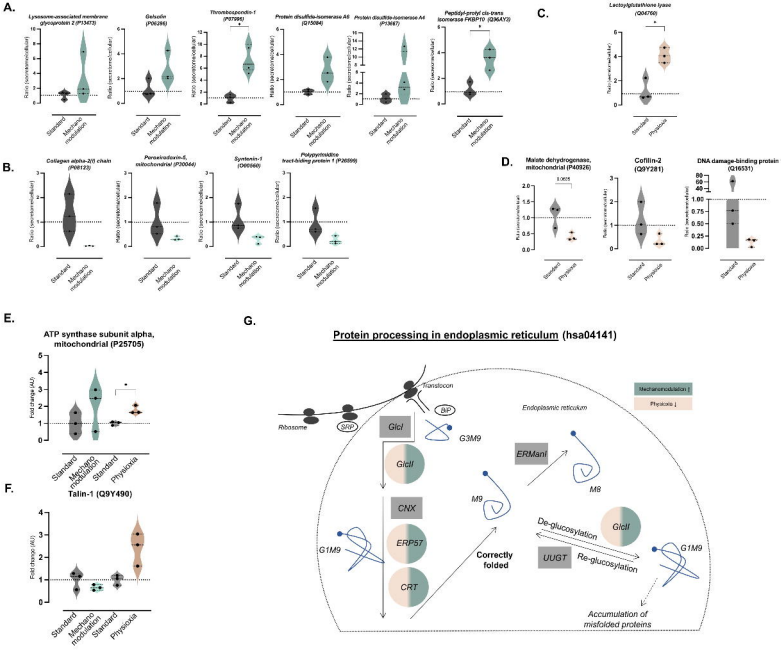
A.
Lysosome-associated membrane glycoprotein 2 (P13473)
Gelsolin (P06396)
Thrombospondin-1 (P07996)
Protein disulfide-isomerase A6 (Q15084)
Protein disulfide-isomerase A4 (P13667)
Peptidyl-prolyl cis-trans isomerase FKBP10 (Q96AY3)
Ratio (normalized value)
Standard
Mechano modulation
B.
Collagen alpha-2(I) chain (P08123)
Peroxiredoxin-5, mitochondrial (P30044)
Syntenin-1 (O00560)
Polypyrimidine tract-binding protein 1 (P26599)
C.
Lactoylglutathione lyase (Q04760)
Physiolo
D.
Malate dehydrogenase, mitochondrial (P40926)
0.0625
Cofilin-2 (Q9Y281)
DNA damage-binding protein 1 (Q16531)
E.
ATP synthase subunit alpha, mitochondrial (P25705)
Fold change (MJ)
F.
Talin-1 (Q9Y490)
G.
Protein processing in endoplasmic reticulum (hsa04141)
Translocon
Ribosome
SRP
BiP
Glcl
G3M9
Glcll
CNX
ERP57
CRT
G1M9
M9
Correctly folded
ERMan1
M8
Endoplasmic reticulum
Mechanomodulation ↑
Physiolo ↓
De-glucosylation
Re-glucosylation
UUGT
Accumulation of misfolded proteins

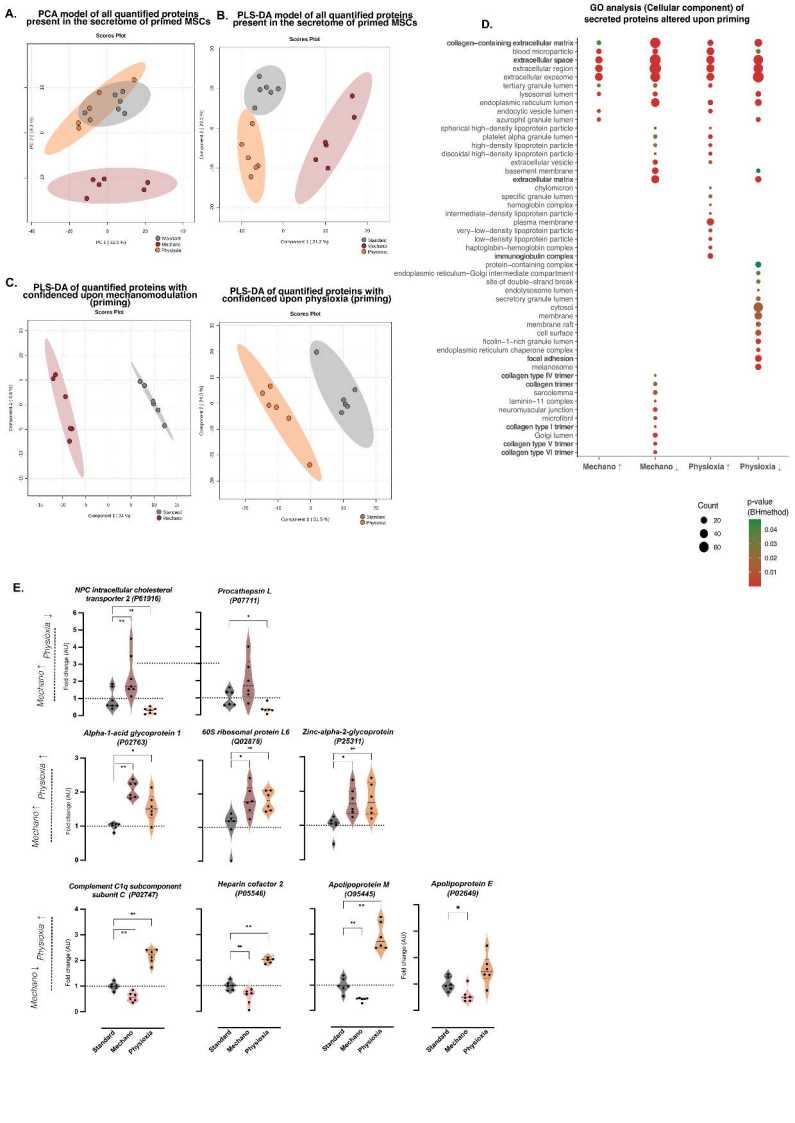
A.
PCA model of all quantified proteins present in the secretome of primed MSCs
Scores Plot
PC 1 (32.5 %)
PC 2 (18.9 %)
Standard
Mechano
Physioxia
B.
PLS-DA model of all quantified proteins present in the secretome of primed MSCs
Scores Plot
Component 1 (71.3 %)
Component 2 (23.0 %)
Standard
Mechano
Physioxia
C.
PLS-DA of quantified proteins with confidenced upon mechanomodulation (priming)
Scores Plot
Component 1 (24 %)
Component 2 (18 %)
Standard
Mechano
PLS-DA of quantified proteins with confidenced upon physioxia (priming)
Scores Plot
Component 1 (31.5 %)
Component 2 (24.5 %)
Standard
Physioxia
D.
GO analysis (Cellular component) of secreted proteins altered upon priming
collagen–containing extracellular matrix
blood microparticle
extracellular space
extracellular region
extracellular exosome
tertiary granule lumen
lysosomal lumen
endoplasmic reticulum lumen
endocytic vesicle lumen
azurophil granule lumen
spherical high–density lipoprotein particle
platelet alpha granule lumen
high–density lipoprotein particle
discoidal high–density lipoprotein particle
extracellular vesicle
basement membrane
extracellular matrix
chylomicron
specific granule lumen
hemoglobin complex
intermediate–density lipoprotein particle
plasma membrane
very–low–density lipoprotein particle
low–density lipoprotein particle
haptoglobin–hemoglobin complex
immunoglobulin complex
protein–containing complex
endoplasmic reticulum–Golgi intermediate compartment
site of double–strand break
endolysosome lumen
secretory granule lumen
cytosol
membrane
membrane raft
cell surface
ficolin–1–rich granule lumen
endoplasmic reticulum chaperone complex
focal adhesion
melanosome
collagen type IV trimer
collagen trimer
sarcolemma
laminin–11 complex
neuromuscular junction
microfibril
collagen type I trimer
Golgi lumen
collagen type V trimer
collagen type VI trimer
Mechano ↑
Mechano ↓
Physioxia ↑
Physioxia ↓
Count
20
40
60
p-value (BHmethod)
0.04
0.03
0.02
0.01
E.
NPC intracellular cholesterol transporter 2 (P61916)
Procathepsin L (P07711)
Alpha-1-acid glycoprotein 1 (P02763)
60S ribosomal protein L6 (Q02878)
Zinc-alpha-2-glycoprotein (P25311)
Complement C1q subcomponent subunit C (P02747)
Heparin cofactor 2 (P05546)
Apolipoprotein M (O95445)
Apolipoprotein E (P02649)
Mechano ↑
Physioxia ↓
Mechano ↑
Physioxia ↑
Mechano ↓
Physioxia ↑
Fold change (AU)
Standard
Mechano
Physioxia

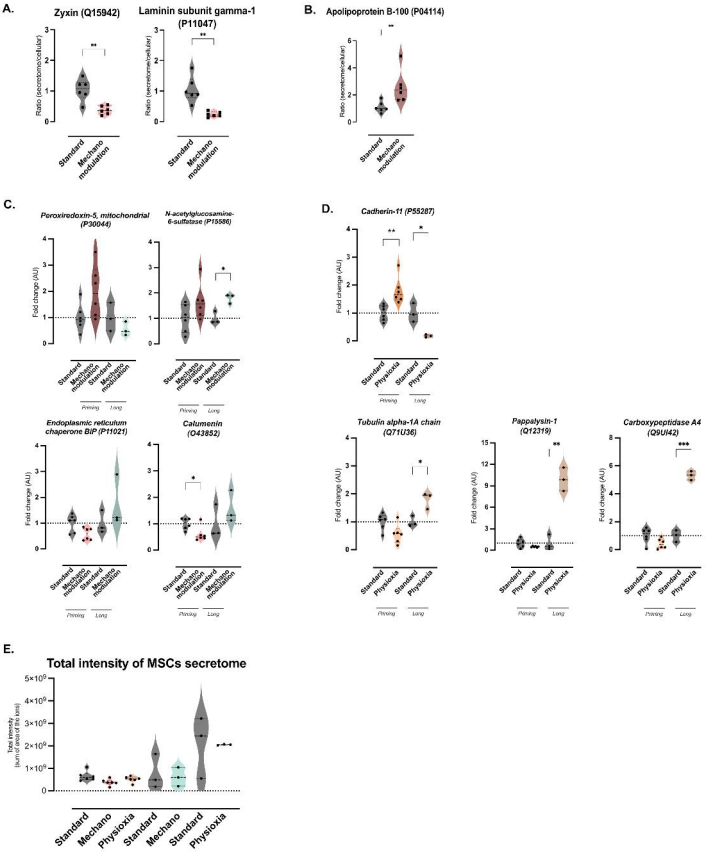
A.
Zyxin (Q15942)
Laminin subunit gamma-1 (P11047)
Ratio (secretomic/cellular)
Standard
Mechano modulation
B.
Apolipoprotein B-100 (P04114)
Ratio (secretomic/cellular)
Standard
Mechano modulation
C.
Peroxiredoxin-5, mitochondrial (P30044)
N-acetylglucosamine-6-sulfatase (P15586)
Endoplasmic reticulum chaperone BiP (P11021)
Calumenin (O43852)
Fold change (AU)
Standard
Mechano modulation
Standard
Mechano modulation
Pinning
Long
D.
Cadherin-11 (P55287)
Tubulin alpha-1A chain (Q71U36)
Pappalysin-1 (Q12319)
Carboxypeptidase A4 (Q9UI42)
Fold change (AU)
Standard
Physioxia
Standard
Physioxia
Pinning
Long
E.
Total intensity of MSCs secretome
Total intensity (sum of area of the loss)
Standard
Mechano
Physioxia
Standard
Mechano
Standard
Physioxia

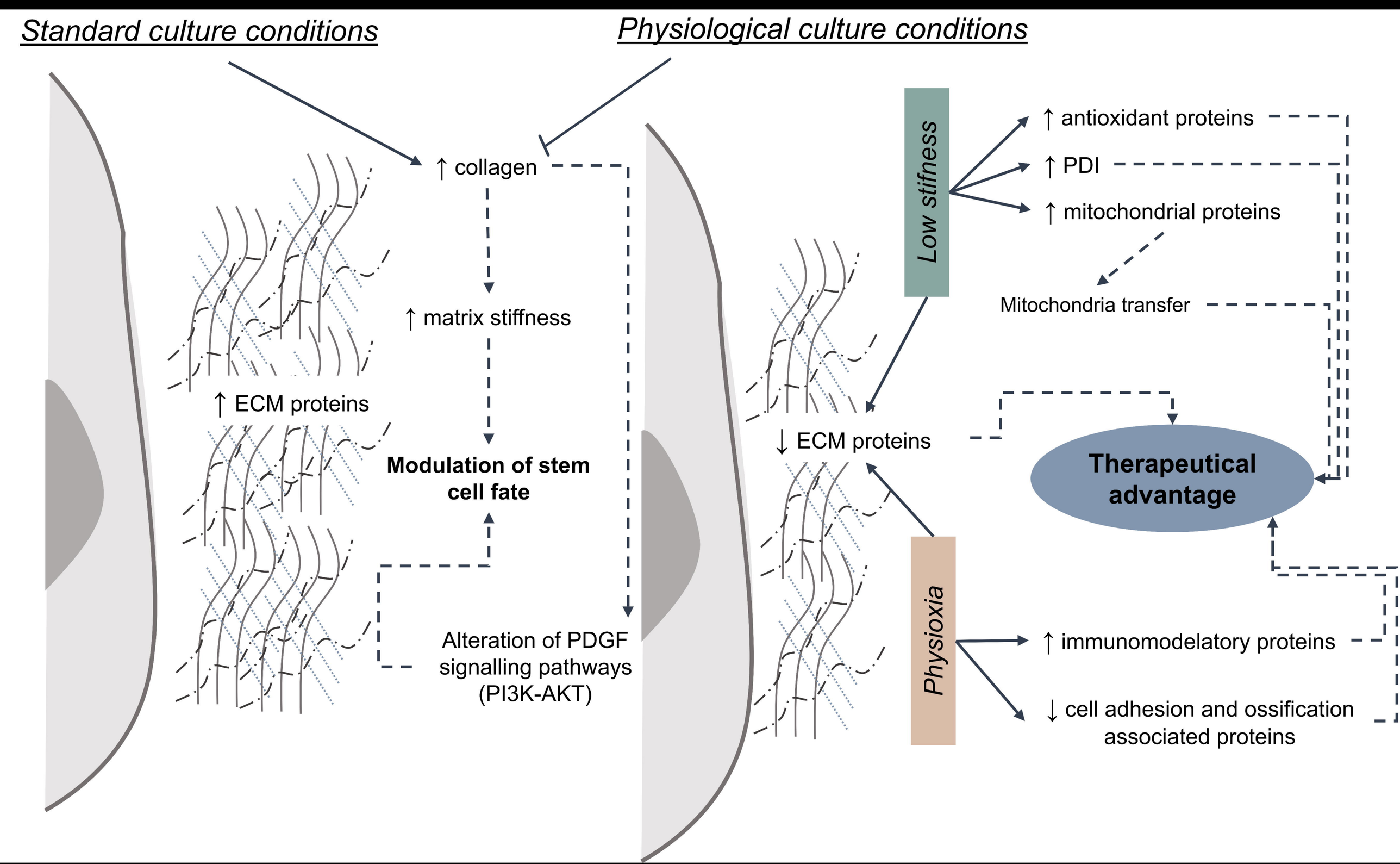
Standard culture conditions
Physiological culture conditions
↑ collagen
↑ matrix stiffness
↑ ECM proteins
Modulation of stem cell fate
Alteration of PDGF signalling pathways (PI3K-AKT)
Low stiffness
↑ antioxidant proteins
↑ PDI
↑ mitochondrial proteins
Mitochondria transfer
↓ ECM proteins
Therapeutical advantage
Physioxia
↑ immunomodelatory proteins
↓ cell adhesion and ossification associated proteins